2007年 2月

碩士學位論文

Action Mechanism of Antimicrobial peptide, Pseudin-2 from *Pseudis paradoxa*

朝鮮大學校 大學院

生物新素材學科

鄭 贊 永

Action Mechanism of Antimicrobial peptide, Pseudin-2 from *Pseudis paradoxa*

***pseudis paradoxa*에서 분리된 항균펩타이드 Pseudin-2의 작용기작에 대한 연구**

2007年 2月 日

朝鮮大學校 大學院

生物新素材學科

鄭 贊 永

Action Mechanism of Antimicrobial peptide, Pseudin-2 from *Pseudis paradoxa*

指導敎授 咸 京 洙

이 論文을 理學碩士 學位申請 論文으로 提出함.

2006年 11月 日

朝鮮大學校 大學院

生物新素材學科

鄭 贊 永

鄭贊永의 碩士學位論文을 認准함

委員長　朝鮮大學校 敎授　　印

委　員　朝鮮大學校 敎授　　印

委　員　朝鮮大學校 敎授　　印

2006年　11月　日

朝鮮大學校 大學院

TABLE OF CONTENTS

LIST OF TABLES

LIST OF FIGURES

초 록

*Pseudis paradoxa*에서 분리된 항균펩타이드 Pseudin-2의 작용기작에 대한 연구

정찬영

지도교수: 함 경 수

조선대학교 대학원

생물신소재 학과

개구리(*Pseudis paradoxa)*의 피부에서 항균 펩타이드인 Pseuin-2를 분리하였다. 24개의 아미노산 잔기(GLNALKKVFQGIHEAIKLINHVQ)로 구성된 항균 펩타이드 pseudin-2는 넓은 범위의 항균 활성을 가지는 반면 상대적으로 낮은 세포독성을 나타냈다. 이 펩타이드는 세포막에 pore를 형성하여 항균 활성을 나타낼 것으로 추정된다.

본 연구에서는 미생물과 인공 지질 막에서 pseudin-2의 작용기작에 대해 연구를 수행하였다. Circular dichroism(CD) 분석을 통해 pseudin-2의 α-helical 구조가 중성 전하를 나타내는 인공 지질 막보다 음 전하를 갖는 인공 지질 막에서 증가하는 것을 확인하였다. 항균활성에 영향을 주었던 염은 펩타이드의 구조적 변화에는 영

향을 주지 못하였다. 따라서 염은 펩타이드에 영향을 주지 않는 반면, 막 전위 에너지에 영향을 주는 것으로 추정된다.

Pseudin-2와 liposomes과의 반응에서 음 전하의 인공 지질 막과 중성 전하의 인공 지질 막 모두에 영향을 주었고, 지질 막 구성성분에 따라 펩타이드의 작용 기작이 다르게 나타났다. 더욱이 pseudin-2는 중성 전하의 인공 지질 막에서 oligomeric 형태를 나타내었다. Psedin-2는 형광 물질을 크기 의존적으로 활성을 나타내었고 중성 전하를 갖는 인공 지질 막에서는 대조군 펩타이드로 사용된 melittin보다 pore의 크기가 큰 것으로 확인되었다. 전자 현미경으로 pseudin-2에 의한 미생물과 인공 지질막의 형태변화를 관찰하였다. 최종적으로 중성 전하의 인공 지질 막에서 pseudin-2는 oligomerization을 통해 toroidal pore기작을 나타내었고, 반면에 음 전하의 인공 지질 막에서는 barrel-stave 작용기작을 나타내었다.

Abstract

Action Mechanism of Antimicrobial peptide, Pseudin-2 from *Pseudis paradoxa*

Jeong, Chan-Young
Supervisor : Prof. Hahm, Kyung-Soo, Ph. D.
Department of Bio-Material Engineering,
Graduate School of Chosun Univercity

Pseudin-2 was isolated from an extract of the skin of the paradoxical frog *pseudis paradoxa* (Pseudidae). Pseudin-2, a naturally occurring 24 residues antimicrobial peptide (GLNALKKVFQGIHEAIKLINHVQ), had broad-spectral antimicrobial activity and relatively low cytotoxicity. This peptide was believed to exert its antimicrobial activity *via* formation of pores in the target cell membrane.

In this study, The mechanical action of pseudin-2 on microorganisms and artificial model membranes were investigated. Circular dichroism (CD) studies showed that Pseudin-2 has an more amphipathic α-helical structure in negative liposome than in zwitterionic liposome. The peptide had no structural change in the increased salt concentration which affected in antimicrobial activity. Therefore, it was found that salt did not affect to peptide conformation but did to membrane potential energy.

A study of interaction of pseudin-2 with several liposomes revealed that it causes perturbation of bilayer integrity of both neutral and negatively charged membranes and that the action of peptide is modulated to some extent by membrane lipid composition. In addition, pseudin-2 formed self-associated oligomeric structure in zwiterionic liposome. It also confirmed be found that the release of fluorescent markers caused by pseudin-2 was size-dependent and it formed larger pore than that by melittin used as a control peptide on the zwitterionic liposome. It was also confirmed that pseudin-2 gave a rise to effect morphological changes of microorganisms and liposomes using electron microscopy. In conclusion, the data presented in this study show that oligomerization of pseudin-2 is required for pore formation which follows the toroidal pore-forming mechanism in zwittrerionic liposome and barrel-stave model in negatively charged liposome.

Ⅰ. Introduction

Antimicrobial peptides are evolutionarily ancient weapons. Their widespread distribution throughout the animal and plant kingdoms suggests that antimicrobial peptides have served a fundamental role in the successful evolution of complex multicellular organisms [1]. Currently, data bases report over 800 sequences for natural antimicrobial peptides and proteins, whereas several thousand others have been designed *de novo* and produced synthetically. Many are positively charged, adopt an amphipathic structure when they are in contact with biological membrane, and act through a non-receptor mediated membrane lytic mechanism. However, recent studies suggest other targets as well. Furthermore, because they act rapidly against various targets, including Gram-negative and Gram-positive bacteria, fungi, enveloped viruses, parasites, and even tumor cells, with a direct and destructive mode of action, they can escape the mechanisms involved in drug resistance, although there is some evidence that specific resistance might occur. Therefore, antimicrobial peptides have been extensively studied for their potential use as antibiotics with new target and attracted increasing research and clinical interest [2].

Amphibian skin has proved to be an especially rich source of such peptides [3]. The synthesis of peptides with antimicrobial activity in granular glands located in the skin is a feature of several anuran (frog and toad) species: Pipidae *Xenopus* [4], Discoglossidae *Bombina* [5, 6], Hyperoliidae *Kassina* [7], Ranidae *Rana* [8, 9], Hylidae *Phyllomedusa* [10], *Agalychnis* [11], and *Litoria* [12], and Myobatrachidae *Uperoleia* [13]. Several classes of peptides have emerged including the following: (Ⅰ) linear peptides free of cysteines and often with an amphipathic sequence; (Ⅱ) peptides with disulfide bonds that can produce a flat dimeric β-sheet structure; and (Ⅲ) peptides with an unusual bias toward certain amino acids, such as proline, arginine, tryptophan, or histidine[4, 14-16]. They are believed to kill the target cell by destabilizing the

ordered structure of the cell membrane *via* either a "barrel stave", "carpet" and "toroidal-pore" models.

In the "barrel stave" model, peptide helices form a bundle in the membrane with a central lumen, much like a barrel composed of helical peptides as the staves. The hydrophobic peptide regions align with the lipid core region of the bilayer and the hydrophilic peptide region form the interior region of the pore [17]. Peptide assembly can occur on the surface or within the hydrophobic core of the membrane, since hydrophobic peptides can span membranes as monomers [18]. Therefore such monomers must associate on the surface of the membrane before insertion and the inserted peptides associated in membranes such that their non-polar side chains face the hydrophobic lipid core of the membrane and the hydrophilic surfaces of peptides point inward into the water-filled pore.

In the "carpet model", peptides accumulate on the bilayer surface. Peptides are electrostatically attracted to the anionic phospholipid head groups at numerous site covering the surface of the membrane in a carpet-like manner. At high peptide concentrations, surface-oriented peptides are thought to disrupt the bilayer in a detergent-like manner, eventually leading to the formation of micelles [19]. At a critical threshold concentration, the peptides from toroidal transient holes in the membrane, allowing additional peptides to access the membrane. Finally, the membrane disintegrates and forms micelles after disruption of the bilayer curvature [20].

In the "toroidal-pore model", antimicrobial peptide helices insert into the membrane and induce the lipid monolayers to bend continuously through the pore so that the water core is lined by both the inserted peptides and the lipid head groups [21]. The lipids in these openings then tilt from the lamellar normal and connect the two leaflets of the membrane, forming a continuous bend from the top to the bottom in the fashion of a toroidal hole; the pore is lined by both the peptides and the lipid head groups, which are likely to screen and mask cationic peptide charges. The toroidal model differs from the barrel-stave model as the peptides are always associated with the lipid head groups even they are perpendicularly inserted in the lipid bilayer [17].

The purpose of the present study was to contribute to our understanding of the membrane activity and specificity of pseudin-2 (GLNALKKVFQGIHEAIKLINNHVQ). Pseudin-2 is an antimicrobial peptide with 24 amino acids, and was first isolated from an extract of the skin of the paradoxical frog, Hylidae (*pseudis paradoxa*) [22]. A *Schiffer-Edmundson* helical wheel projection [23] of its structure indicates to amphipathic peptide with the hydrophilic residues Lys^{6}, Lys^{7}, Glu^{14} and Lys^{17} segregating on one face and the hydrophobic residues Leu^{2}, Leu^{5}, Val^{8}, Phe^{9}, Ile^{12}, Ile^{16} and Val^{23} segregating on the opposite face (Figure. 1). Pseudin-2 has broad-spectrum antimicrobial activity such as melittin but it has less cytotoxicity than melittin against HaCaT Cell and NIH/3T3 Cell more than melittin. A study of interaction of pseudin-2 with several liposomes revealed that it causes perturbation of bilayer integrity of both neutral and negatively charged membranes and that the action of peptide is modulated to some extent by membrane lipid composition. In addition, pseudin-2 formed self-associated oligomeric structure in zwiterionic liposome. We also performed that the release of fluorescent markers caused by pseudin-2 was size-dependent and it formed larger pore than melittin, used as control peptide, on the zwitterionic liposome. We confirmed that pseudin-2 effected morphological changes of microorganisms and liposomes by using electron microscopy. The results are discussed in terms of a proposed model for the mode of action of pseudin-2.

Ⅱ. MATERIALS AND METHODS

1. Materials

Bis (sulfosuccinimidyl)suberate (BS^3), chitin, cellulose, chitosan, peptidoglycan (from *S. aureus*), lipopolysaccharide (LPS) (from *E. coli* 0111:B4), bicinchoninic acid (BCA) protein reagent, L-α-phosphatidylethanolamine (PE) (Type V, from *E. coli*), cholesterol (CH), and fluorescein isothiocyanate dextrans of 4, 10, 40, 70 and 500 kDa average molecular mass (FITC-D 4/ 10/ 40/ 70/ 500) were purchased all from Sigma Chemical Co. (St. Louis, MO). Egg yolk$_{L\text{-}\alpha}$-phosphatidyl-$_{DL}$-glycerol (PG) and egg yolk $_{L\text{-}\alpha}$-phosphatidylcholine (PC) were obtained from Avanti Polar Lipids (Alabaster, AL). 3,3`-diethylthio-dicarbocyanine iodide (Dis-C_3-5) and calcein were from Molecular Probes (Eugene, OR). The rest of the reagents were analytical grade.

2. Peptide synthesis

All peptides were synthesized by solid phase methods [24] using Fmoc (N-(9-fluorenyl)methoxycarbonyl)-protected amino acids on a Applied Biosystems Model 433A peptide synthesizer. 4-methyl benzhydrylamine resin (MBHA, Novabiochem) (0.55 mmol/g) was used to produce an amidated C-terminus. For each coupling step, the Fmoc protected amino acid and coupling reagents were added in 10-fold molar excess with respect to resin substitution. Coupling (60-90 min) was carried out with dicyclohexylcarbodiimide (DCC) and 1-hydroxy benzotriazole (HOBT) in the presence of N-methyl-2-pyrrolidone (NMP). Cleavage from resin and deprotection of the synthesized peptide were carried out with a solution of 90% trifluoroacetic acid, 3% water, 1% triisopropylsilane, and 2% each of 1,2-ethanedithiol, thioanisole, and phenol. After repeated precipitation with ether. Labeling at the N terminus of a peptide was achieved by a standard procedure reported earlier [25]. In brief, 15-20 m of

resin-bound peptide was treated with 25% piperidine (in DMF) to remove the Fmoc group from the N-terminal amino group. The resin was washed and dried. Then Fmoc de-protected resin-bound peptides were incubated with tetramethyrhodamine succinimidyl ester in dimethyformamide in the presence of 5% diisopropylethylamine for 48-72 h, which ultimately resulted in the formation of N-Rho-peptides. Similarly, resin-bound peptides were treated with NBD-fluoride to obtain N-NBD-peptide. After sufficient labeling, the resins were washed with DMF and DCM in order to remove the unreacted probe. The peptides were cleaved from the resin as above and precipitated with dry ether. The crude peptide was purified by a reversed-phase preparative HPLC on a Waters 15-μm Deltapak C18 column (19 x 300 mm), using an appropriate 0-60% acetonitrile gradient in 0.1% trifluoroacetic acid. Purity of the purified peptide was checked by the analytical reversed-phase HPLC using a Vydac C18 column (4.6 x 250 mm, 300Å, 5 nm). The molecular masses of the peptides were confirmed with matrix-assisted laser desorption ionization mass spectrometer (MALDI II, Kratos Analytical Ins) [26].

3. Preparation of liposomes

SUVs [27] and LUVs [28] were prepared for dye leakage and binding assays, respectively. The desired mixtures of lipids was dissolved in chloroform, dried in a glass tube under nitrogen, and then lyophilized overnight to obtain a thin lipid film. Then, dry lipid films were resuspended in phosphate buffer (10 mM sodium phosphate containing 10 mM NaCl, pH 7.4) on water-bath at 50℃ and sealed with parafilm under nitrogen. The resulting mixtures were vortexed occasionally to disperse the lipids. To prepare the SUVs, lipid dispersions were sonicated in a bath-type soincated for 5 min in cold water until the turbidity had cleared and then extruded 10 times through polycarbonate membranes with 0.1 μm diameter pores to ensure a homogeneous population. LUVs were prepared by freeze-thawing the desired lipid suspensions five times under nitrogen, and then extruded 10 times through

polycarbonate membranes with 0.4 μm diameter pores to ensure a homogeneous population. Their concentration was determined by a standard phosphate assay, preceded by acid digestion of the phospholipids. The average dimeters of vesicles were confirmed by transmission electron microscopy (FEI Tecnai 12).

4. Antimicrobial assay

(1) Strains

Escherichia coli (ATCC 25922), *Salmonella typhimurium* (KCTC 1926), *Pseudomonas aeruginosa* (KCTC 1637), *Bacillus subtilis* (KCTC 1918), *Staphylococcus epidermis* (KTCT 1917), *Salmonella typhimurium* (KCTC 1926), *Staphylococcus aureus* (ATCC 25923), *Candida albicans* (KCTC 7270), *Trichosporon beigellii* (KCTC 7707), *Aspergillus fumigatus* (KCTC 6145), *Fusarium oxysporum* (KCTC 16909), and *Aspergillus flavus* (KCTC 6905) were supplied by the Korean Collection for Type Cultures (KCTC), Korea Research Institute of Bioscience and Biotechnology (Taejon, Korea).

(2) Antibacterial activity assay

The bacteria were grown to the mid-logarithmic phase in trypticase soy broth at 37℃. The antibacterial activity of each peptide was performed using the microdilution assay. Briefly, bacteria cells were collected in mid-log phase and suspended with buffer I (low ionic strength buffer; 10 mM sodium phosphate, pH 7.2) and buffer II (high ionic strength buffer; phosphate-buffer saline, pH 7.2). Two-fold serial dilutions of each peptide, ranged form 0.5 to 64 μM, in buffer I and II, were arranged in sterile 96-well plates, then an aliquot of cell suspension was added to each well. The cell count was 1×10^6 CFU (colony forming units) / ml. The plates were incubated for 2 hr at 37℃ for fungal cell. At the end of the incubation, 50 μl of

20-fold diluted samples were plated on appropriate agar plates, depending on the microorganism tested. Plates were incubated for 24 hr, and then colonies were counted. The lowest concentration of peptide that completely inhibited growth was defined as the minimal inhibition concentration (MIC). The MIC values were calculated as an average of independent experiments performed in triplicate.

(3) Antifungal activity assay

To determine MIC of peptide against various fungal pathogens, fungal spores from 10-days-old cultures grown on PDA plate at 28°C were collected with 0.08% Triton X-100. Eighty microliters of a spore suspension (final concentration 10^4 spores/ml) in PD media was subjected in 96-well microtiter plates and mixed twenty microliters of peptides, which are appropriately 2-fold serial diluted concentrations. After 12 to 36 h of incubation at 28°C, growth or germination of fungi was evaluated microscopically, using an inverted microscope, and turbidity of each well was also measured by absorbance at 595 nm using a microtiter reader (Molecular Devices Emax, CA, USA).

5. Hemolytic and cytotoxic assay

(1) Hemolytic assay

Hemolytic activities were measured for all peptides and assessed determined sing hRBCs from healthy donor, collected on heparin. Fresh hRBCs were rinsed three times in PBS (1.5 mM KH_2PO_4, 2.7 mM KCl, 8.1 mM Na_2HPO_4, 135 mM NaCl, pH 7.4) by centrifugation for 10 min at 800 × g and resuspended in PBS. The peptides dissolved in PBS were then added to 100 μl of the stock hRBCs solution in PBS (final erythrocyte concentration, 4% v/v). The samples were incubated with agitation for 60 min at 37℃. The samples were then centrifuged at 800 × g for 10 min. The

absorbance of the supernatant was measured at 414 nm, and controls for zero hemolysis (blank) and 100% hemolysis consisted of hRBCs suspended in PBS and 1% Triton X-100, respectively. Each measurement was made in triplicate [29].

% haemolysis = [(Abs_{414} nm in the peptide solution - Abs_{414} nm in PBS) / (Abs_{414} nm in 0.1% Triton-X100 - Abs_{414} nm in PBS)] × 100

(2) Cytotoxic assay

NIH/3T3 (Mouse Fibroblast cells) and HaCaT (Human Keratinocyte cells) were cultivated in Dulbecco's minimal Eagle medium (DMEM) medium at 37℃ and 5% CO_2 for 5-7 days. Assays were performed by incubation of 2×10^3 cells with varying concentration of peptides for 19 h at 37 °C and 5% CO_2 in a 96-well plate. The Triton X-100 (0.1% final concentration) was used as negative control and pure medium assay was used as negative control. Proliferation and viability a was determined by MTT [3-94, (5-dimethylthiazole-2-yl)-2,5-diphrnyl tetrazolium bromide] assay. The plate was then incubated for 24 h before adding to each well 50 μl of MTT reaction solution. The medium containing MTT was removed, and 100 μl of dimethyl sulfoxide (DMSO) was added. Cells were incubated for 10 min 37℃ with gentle shaking. The optical density was read at 550 nm in an enzyme-linked immunosorbent assay plate reader after 2 h of incubation. Cell viability was determined relative to the control. All studies were performed in triplicate.

6. Circular Dichroism (CD) spectroscopy

All CD spectra were recorded using a J-810 pectrophotometer (Jasco, USA) Spectral scans were performed from 190 and 250 nm, with a step resolution of 0.1 nm and bandwidth of 1.0 nm at 50 nm/min. A 0.1 cm-pathlength quartz optical was used for the measurements and values from 5 scans were averaged per sample. The

peptides were scanned as 30 μM solutions in appropriate buffers with and/or not NaCl and in the presence of various liposomes [30, 31].

7. Peptide binding to microbial cell wall components

To perform an *in vitro* binding assay of synthetic peudin-2 and melittin, we used Curdlan (β-1, 3-glucan; yeast), peptidoglycan (β-1, 4-glycosidic linkage between N-acetylmuramic acid and N-acetylglucosamine; Gram-positive bacteria), chitin (β-1, 4-N-actyl-D-glucosamine) and cellulose (β-1, 4-glucan). The synthetic peptides were suspended with 10 mM sodium phosphate, pH 7.4. Insoluble polysaccharide (200 μg) were added to a 200 μl aliquot of peptides solution (5 μg) and incubated at room temperature with mild agitation for 30 min. The mixture were centrifuged (12,000 × g for 20 min) and the resulting pellet was washed three times with 0.5 ml of washing buffer (10 mM Tris, pH 7.5, 500 mM NaCl, 0.02% Tween 20). The peptides bound to the insoluble polysaccharide were detached by adding SDS-PAGE sample buffer and then subjected to 16.5% Tricine SDS-PAGE. The LPS (Gram-negative bacteria) binding assay was carried out using essentially the same method as described above, except for centrifugation at 22,000 × g for 15 min due to precipitate small liposomes of LPS [32].

8. Determination of peptide detergent-like action on liposomes

To evaluate the bilayer-disruptive property of pseudin-2 and melittin, the change in attenuance at 405 nm of liposome suspensions was measured upon incubation with pseudin-2 and melittin. Clearing of the turbid vesicle suspension indicates the solubilization of liposomes into smaller particles. LUVs suspensions in 10 mM sodium phosphate, pH 7.4, were incubated with increasing amounts of either pseudin-2 or melittin at room temperature for 30 min. After this time, attenuance of

samples were measured on a ELISA at 405nm. Controls contained liposomes but no peptides. Measurements were made in triplicate.

9. Oligomerization of the peptides in solution

Rhodamine-labelled peptide (0.1 μM final con.) was added to 2 ml of 10 mM Sodium Phosphate buffer, and rhodamine fluorescence emission was monitored. Proteinase K (10 μg / ml) was then added, resulting in an increase in the fluorescence emission as a result of the dequenching of the rhodamine fluorescence. More proteinase K was added until no further increase in the fluorescence emission was observed. Excitation was set at 530 nm (10 nm slit) and emission was set at 582 nm (8 nm slit). All subsequent fluorescence measurements were performed at room temperature on a Perkin-Elmer LS-55 luminoscence spectrometer.

10. Accessibility of membrane-bound peptides to proteolytic degradation

Lipid vesicles (150 μM in a 1 ml cuvette) were added to NBD labeled peptides (0.1 μM, in 10 mM Sodium Phosphate buffer). After 15 min, proteinase K (10 μg / ml) was added. Fluorescence emission as a function of time was recorded before and after the addition of the enzyme. In control experiments, NBD-labeled peptides were pre-incubated with proteinase K in aqueous solution, followed by the addition of the liposomes. Fluorescence measurements were performed with excitation set at 470 nm (10 nm slit) and emission set at 530 nm (8 nm slit).

11. Chemical cross-linking analysis

Pseudin-2 and melittin were incubated with LUVs for 10 min at room temperature.

The samples were further incubated with 80 μM of BS^3 [33] and for 1 hr. After incubation, the samples were added to a tricine sample buffer (1 ml 1M Tris-HCl pH 6.8, 0.4 g SDS, 2 ml glycerol, 0.02 g bromophenol blue and 0.31 g DTT adjust volume to 20 ml) and subjected to 16.5% Tricine-SDS-PAGE without heating. The peptide bands were identified in the gels following Coomassie Brilliant Blue G-250 staining.

12. Fluorescence resonance energy transfer analysis

Fluorescence energy transfer experiments were performed with excitation wavelength set at 467 nm and emission range of 500-600 nm. Desired amount of the NBD-labeled peptide was taken in a fluorimeter cuvette. Sufficient amounts of the phospholipid vesicles were added to the NBD-labeled peptide to ensure that the peptides were bound to the membrane. Now Rho-labeled acceptor peptide was added to the donor peptide-lipid complex. Energy transfer from donor to acceptor was determined by subtracting the acceptor fluorescence in the presence of lipid and unlabeled donor from the fluorescence signal obtained in the presence of donor, acceptor and lipid vesicles.

13. Membrane potential depolarization assays

(1) depolarization assay with liposomes

The ability of the peptides to destabilize the phospholipid bilayer was detected by their efficacy to dissipate the diffusion potential across the membrane. The experiments were performed as follows [34, 35]. Lipid vesicles were prepared in K^+ buffer (50 mM K_2SO_4/25 mM HEPES sulfate, pH 6.8). Required amounts of the lipid vesicles were mixed with isotonic (K^+-free) Na^+ buffer (50 mM Na_2SO_4/25 mM

HEPES sulfate, pH 6.8) followed by the addition of the potential sensitive dye diS-C_3-5. Addition of valinomycin created a negative potential inside the lipid vesicles by the selective efflux of K^+ ions from the lipid vesicles. As a result of that a quenching of the fluorescence of the dye occurred. When the dye exhibited a steady fluorescence level, peptides were added. Membrane permeability of the peptide was detected by the increase in fluorescence, which resulted from the dissipation of diffusion potential. Fluorescence was monitored at 670 nm with respect to time (s) with excitation wavelength of 620 nm. The peptide-induced dissipation of diffusion potential was measured in terms of percentage of fluorescence recovery (F_t) as defined by Refs. 25 and 36 in Equation ,

$$F_t = [\ (I_t - I_0)\ /\ (I_f - I_0)\ ] \times 100\%$$

where I_t = the observed fluorescence after the addition of a peptide at time t (10 min after the addition of the peptide), I_0 = the fluorescence after the addition valinomycin and I_f = the total fluorescence observed before the addition of valinomycin.

(2) Depolarization assay with bacteria

The assay was performed with whole cells of Gram-positive and Gram-negative bacteria and spheroplasts of Gram-negative bacteria using the experimental conditions described previously [37].

Gram-positive Bacteria — *S. aureus* was grown at 37 °C with agitation to mid-log phase (OD_{600} = 0.4). The cells were centrifuged and washed once with buffer (20 mM glucose, 5 mM HEPES, pH 7.3) and resuspended to a OD_{600} of 0.05 in a similar buffer containing 0.1 M KCl. The cells (the same concentration as in the biological activity assay) were incubated with 1 μM diS-C_3-5 until a stable reduction of fluorescence was achieved (around 60 min), indicating the incorporation of the dye into the bacterial membrane. The peptides were then added from the stock solution (1

mg / ㎖) and dissolved in the KCl buffer to achieve the desired concentration (0.1-10 fold the MIC concentration). Membrane depolarization was monitored by observing the change in the intensity of fluorescence emission of the membrane potential-sensitive dye diS-C_3-5 (excitation wavelength λex = 622 nm, emission wavelength λem = 670 nm) after the addition of different concentrations of peptides.

Gram-negative Bacteria — Spheroplasts of *E. coli* (lipopolysaccharide and peptidoglycane free bacteria [38]) were prepared by osmotic shock procedure as follows. First, the cells from cultures grown to OD_{600} = 0.8 were harvested by centrifugation and washed twice with 10 mM Tris/H_2SO_4, 25% sucrose, pH 7.5. Next, the cells were resuspended in the washing buffer containing 1 mM EDTA. After a 10-min incubation at 20°C with rotary mixing, the cells were collected by centrifugation and resuspended immediately in freezing (0°C) water. After a 10-min incubation at 4°C with rotary mixing, the spheroplasts were collected by centrifugation. The spheroplasts were then resuspended to OD_{600} of 0.05 in a buffer containing 20 mM glucose, 5 mM HEPES, 1 M KCl, pH 7.3. Further treatment was done exactly as described for *S. aureus*.

14. Calcein leakage from lipid vesicles

Peptide induced release of calcein from calcein-entrapped vesicles is often employed to detect the pore-forming activity of proteins and peptides. Calcein-entrapped lipid vesicles were prepared with a self-quenching concentration (60 mM) of the dye in 10 mM HEPES at pH 7.4 as reported earlier [39, 40]. Briefly, thin film of lipid (either PC/CH or PE/PG) was resuspended in calcein solution, vortexed for 5 min and then sonicated in a bath-type sonicator. The non-encapsulated calcein was removed from the liposome suspension by gel filtration using a Sephadex G-50 column. Usually lipid vesicles are diluted to 10-fold after passing through a Sephadex G-50 column. The eluted calcein-entrapped vesicles were diluted further in

the same buffer to a final lipid concentration of 3.0 μM for the experiment. Peptide-induced release of calcein from the lipid vesicles was monitored by the increase in fluorescence due to the dilution of the dye from its self-quenched concentration. Fluorescence was monitored at room temperature with excitation and emission wavelengths fixed at 490 and 520 nm, respectively. Calcein release as measured by the fluorescence recovery is defined by the same equation as used to determine the dissipation of diffusion potential. However, in this case If, the total fluorescence, was determined after the addition of Triton X-100 (0.1% final concentration) to the dye-entrapped vesicle suspension.

15. Dextran leakage from lipid vesicles

Dextran-loaded vesicles containing the FITC-D of choice (FITC-D 4, 10, 40, 70, and 500) were prepared as reported elsewhere [41]. The release of dextran from loaded vesicles upon interaction with pseudin-2 and melittin were examined fluorimetrically; excitation and emission wavelengths were 494 nm and 520 nm respectively. In a typical experiment, an aliquot of the peptide solution in 20% (v/v) ethanol was incubated with a suspension of dextran-loaded vesicles in buffer, with a final lipid concentration of 50 μM. The mixture (2 ml, final volume) was stirred gently for 10min in the dark and then centrifuged at 22500 × g for 30 min. The supernatant was recovered and its fluorescence intensity recorded. The maximum fluorescence intensity was determined by the addition of 20 μl of 10% (v/v) Triton X-100 to the vesicle suspension. Dextran release as measured by the fluorescence recovery is defined by the same equation as used to determine the calcein leakage.

16. Electron microscopy assay

(1) Confocal laser-scanning microscopy

In order to analyze cellular distribution of Rhodamine (Rho) labeled pseudin-2, confocal laser scanning microscopy was used. *E. coli*, *S. aureus* and *C. albicans* were inoculated into 3 ml of each medium and incubated at 37°C and 28°C for 12 h. The cells were then diluted 1:50 in Saubouraud dextrose broth medium (SDB medium; 1% bacto peptone, 4% glucose) and incubated at 28°C for 3 h to enrich the population of exponentially growing cells. The number of cells was adjusted to 10^6 cells per milliliter by diluting in the SB medium. In some cases, the stationary-phase cells were used instead of the exponential-phase cells. Rho-pseudin-2 was added to 100 μl of the cell suspension at 6.25 μM, and the cells were incubated at 37°C and 28°C for 20 min. The cells were pelleted by centrifugation at 6,000 rpm for 5 min and washed three times with ice-cold PBS buffer. Extracellular localization of Rho-pseudin-2 was examined by LSM510-META microscope (ZIESS).

(2) Scanning electron microscopy (SEM)

Mid-log growth phase S. aureus, E. coli and C. albicans were resuspended at 10^8 C.F.U./ml in sodium-phosphate buffer, pH 7.4, supplemented with 100 mM NaCl, and incubated at 37℃ and 28℃, respectively, pseudin-2 and melittin. Controls were run in the absence of peptide solution. After 30 min the cells were fixed with an equal volume of 5% (v/v) glutaraldehyde in 0.2 M sodium-cacodylate buffer, pH 7.4. After fixation for 2 h at 4℃, the samples were filtered on isopore filters (0.2 μm pore size, Millipore, Bedford, MA) and extensively washed with 0.1 M cacodylate buffer, pH 7.4. The filters were then treated with 1% (w/v) osmium tetroxide, washed with 5% (w/v) sucrose in cacodylate buffer and subsequently dehydrated with a graded ethanol series. After lyophilization and gold coating, the samples were examined on a HITHACHI S-2400 instrument (HITHACHI, Japan) [42].

(3)**Transmission electron microscopy (TEM)**

Pseudin-2 and melittin were incubated with SUVs at room temperature in 10 mM sodium phosphate buffer. After incubation, peptides were applied to glow-discharged carbon-coated copper grids. After allowing the peptide and SUVs to absorb for 1 min, the grids were rinsed with the same buffer , and stained with 2% (w/v) uranyl acetate. Electron micrographs were then recorded (FEI Technei 12 microscope) at nominal magnifications (67 000-110,000 $\times_{gav}$) and an accelerating voltage of 120 kV [42].

Ⅲ. RESULTS

1. Antimicrobial activity and cytotoxicity of pseudin-2

Pseudin-2 was analyzed for its potential, that inhibit the growth of bacteria, yeast and fungi compare to melittin (table 1). Pseudin-2 had more a potent antibiotic activity against bacteria more than yeast and fungi, and it showed a similar activity with melittin, used as a control peptide, in different ionic strength buffer.

Cytotoxicities of pseudin-2 and melittin in the three cell lines were compared, RBCs (Human Red Blood Cells), NIH/3T3 (Mouse Fibroblast cells), HaCaT (Spontaneously immortalized Human Keratinocyte cells). Pseudin-2 showed relatively low hemolytic activity, whereas melittin exerted a strong hemolytic activity (Table 2). Melittin also exhibited a strong cytotoxicity activity against NIH/3T3 and HaCaT cells. Melittin has been known as one of most potent antimicrobial peptide (AMP) but has a strong cytotoxic activity which can lead to serious problems on *in vivo* applications. But, pseudin-2 has comparative high antimicrobial activity and relatively low cytotoxicity. Comparing selectivity of peptides against bacterial cells and mammalian cells, We suggest that pseudin-2 is a better AMP than melittin.

2. Secondary Structure of pseudin-2

To examine the secondary structure of the pseudin-2, we performed its CD measurements in different solutions. As shown in Figure 2A, pseudin-2 formed concentration-dependently helical conformation significantly, which has lower ellipticity at 208 nm and 222 nm. These result indicates that amino acids of each peptides was induced from random coil to amphipathic α-helical structure, because the increasing peptides may make a hydrophobic environment as one peptide is closed to another by

increasing concentration of peptide. In the more hydrophobic solvent (50% trifluoroethanol), the negative bands centered at 208 and 222 nm and the positive band centered at 193 nm are indicative of significant α-helical character. Interestingly, although antimicrobial activity of pseudin-2 was affected by ion strength as salt, its structure did not change when the peptides were incubated in a buffer with an NaCl concentration of up to 100 mM (Figure. 2C). To simulate the contact of the peptides with microorganism membrane, we incubated the pseudin-2 with unilamellar vesicles having different compositions. It is induced to helical structure in the presence of liposomes, although to different extents, that is similar to hydrophobic solvent. Its helicity was increased in the negatively charged vesicles more than zwitterionic vesicles due to electrostatic interaction between positively charged amino acids of peptide and head groups of negatively charged lipid.

3. Target of pseudin-2 confirmed by confocal laser-scanning microscopy

To determine the site of action of the pseudin-2, Rho-labeled peptide was incubated with *E. coli*, *S. aureus* and *C. albicans* and their localization were visualized by confocal laser-scanning microscopy. Figure 3 shows that Rho-labeled pseudin-2 bound on bacterial cell surfaces and bound on and penetrated into yeast cells. Therefore, we performed next experiment which focus to cell surfaces (cell wall and membrane).

4. Effective pseudin-2 recognize the chitin and peptidoglycan

To evaluate the binding specificity of pseudin-2 to microbial cell wall components, various insoluble oligosaccharide polymers (such as β-1,3-glucan and chitin from yeast, LPS from Gram-negative bactria, peptidoglycan from Gram-positive

bacteria, chitosan and celullose) was used. After incubation, the peptides bound to the insoluble polymers were extracted using an SDS-PAGE sample buffer and confirmed by SDS-PAGE. As shown in Figure 4, pseudin-2 bound to chitin and peptidoglycan but did not interact with LPS, which is comparable with result of melittin as previous report [48]. The binding ability in peptidoglycan more predominated than in chitin. These results is consistent with previous antimicrobial activity assay, in which pseudin-2 has a better antibiotic activity against bacterial cells than fungal cells. But, all can not be described by only this result due to different cell wall conponents of gram-negative and -positive bacteria.

5. Effects of pseudin-2 to liposomes disruption

Several α-helical peptides, including melittin and magainins, are known, at high peptide concentrations, to solubilize membranes in a detergent-like manner, causing both bilayer micellization and fusion [49, 50]. In order to investigate effects of pseudin-2 toward membranes, its another target, we measured the attenuance of artificial LUVs with various compositions. Peptide distribution in changes of vesicle size resulting from peptide-induced aggregation or micellization can be monitored by following the attenuance of the liposome suspension. The changes in the peptide to lipid molar ratio are shown in Figure 5, which were compared with melittin, used as a reference. Pseudin-2 did not caused aggregation of neutral and negative vesicles, whereas the melittin aggregated a negatively charged vesicles in dose-dependent manner.

6. Pseudin-2 self-associates in solution

The ability of pseudin-2 to self associate in solution was investigated using Rho-labelled peptides. Rho-labelled melittin was used as a control peptide. The fluorescence of rhodamine is only slightly sensitive to the polarity of its environmental

and therefore it can studied in solution. This assay is based on the principle that the fluorescence is quenched when several rhodamines are in close proximity, i.e., when they self-associate or form oligomers. The fluorescence of the respective peptide at different concentrations is compared to the fluorescence of the peptide after treatment with proteinase K, which resulted in total degradation of the peptides. The percentage of fluorescence recovery in solution is a measurement of the aggregation state. Figure 6 showed that the initial fluorescence of Rho-pseudin-2 is lower than that of Rho-melittin, which suggests a higher oligomeric state for pseudin-2 compared with melittin. After 2 hr of treatment with proteinase K, which resulted in total degradation of the peptides, the fluorescence intensity of all the peptide reached similar values. This indicates that pseudin-2 can self-associate like to melittin.

7. Pseudin-2 self-assembles in lipid vesicles

To further evaluate whether the observation described above indeed reflected self-association in lipid vesicles, we performed the fluorescence resonance energy transfer with the peptides labelled by NBD as fluorescence energy donor and rhodamine as energy acceptor. Two probes fulfill the spectroscopic criteria of fluorescence resonance energy transfer when they are in close proximity, and the assembly of a peptides can be determined with the help of energy transfer experiment between its NBD and rodamine labelled peptides. In the presence of lipid vesicles (400 μM), addition of Rho-pseudin-2 (final concentration of 0.05-0.4 μM) to NBD-pseudin-2 (0.2 μM) quenched the donor's emission and increased the acceptor's emission, which is consistentent with energy transfer (Figure 7A, B). As shown in the panel A of figure 7, the addition of energy acceptor Rho-pseudin-2 to donor NBD-pseudin-2 onto zwitterionic liposome resulted in an appreciable decrease in NBD fluorescence concomitant with the increase in rhodamine fluorescence. This observation was consistent with the energy transfer from NBD-pseudin-2 to Rho-pseudin-2. This suggests that pseudin-2 self-assembled in PC/CH (zwitterionic) liposomes. The panel B

of figure 7 depicts the results of energy transfer experiments between NBD-pseudin-2 and Rho-pseudin-2 in PE/PG (negatively charged) liposome. In contrast to zwitterionic liposome, fluorescence of the donor peptide little decreased . These result suggest that pseudin-2 did weakly self-assemble in PE/PG (negatively) liposomes. Panel C, D of figure 7 shown that melittin self-assembled in both PC/CH (zwitterionic) and PE/PG (negatively) liposomes.

We examined oligomeric states of pseudin-2 using chemical cross-linking in the lipid vesicles. As shown in Figure 8, in PC/CH (B, C, D) liposomes, multimeric complexes of pseudin-2 were observed, and pseudin-2 exists to trimer in PE/PG liposomes.

8. Organization of the peptides upon binding to vesicles

In order to determine the location of the peptides onto the membrane, proteolytic cleavage experiments were performed with NBD-labelled peptides in their membrane-bound state. The basis of this experiment is that NBD-labelled peptides, bound onto the membrane-surface, are cleaved by a proteolytic enzyme like proteinase K, which can be monitored by the decrease in NBD-fluorescence from the characteristic membrane-bound level. On the other hand, NBD-fluorescence of a membrane-inserted peptide is not be decreased because proteinase K is not be accessible in membrane. Figure 9(A) shows that, after proteinase K treatment, the fluorescence of the NBD-labelled pseudin-2 did not decrease (a, b, c). This result indicates that at least a part of the peptide was hidden inside the lipid bilayer and hence not cleaved after incubation. Whereas, the fluorescence of NBD decreased when pseudin-2 added in PC/CH (d). This indicates that the pseudin-2 bound to PC/CH is susceptible to degradation. Control experiment was done by adding proteinase K to NBD-labelled peptide prior to the addition of vesicles (Figure 9B). Melittin is the case with control experiment, when vesicles were added to the partially degraded peptide, a smaller increase in fluorescence was observed due to binding of the partially uncleaved

peptide to vesicles. The finding that NBD-pseudin-2 did not protected from degradation when bound to PC/CH vesicles, is different from the results found with melittin. We suggests that pseudin-2 is not inserted but just bound in zwitterionic liposome and inserted in negatively charged liposome. This indicates that it might be bound in eukaryotic membrane and inserted in prokaryotic membrane, and that consistent with the results of its antimicrobial activity.

9. Depolarization of the membrane potential of bacteria and liposomes

To further investigate how their interaction with the bacterial plasma membrane leads to cell death, we assessed the ability of the peptides to induce membrane depolarization in intact bacteria and *E. coli* spheroplasts (Figure 10). The cell concentrations in the diffusion potential assay were similar to that used in the antimicrobial assay. Figure 10 shows the dose-dependent dissipation of the transmembrane potential of bacteria by peptides. The results reveal a direct correlation between the MIC values for them. The depolarization effects of pseudin-2 are almost similar to both outer membrane (intact cells) and inner membrane (*E. coli* spheroplast), but especially melittin was more sensitive in intact *E. coli* than *E. coli* spheroplasts. It is reasonable to deduce that the major targets of pseudin-2 are both membranes and that of melittin is the outer membrane of the bacteria. Therefore, pseudin-2 is more effective than melittin against bacterial strains.

Dissipation of diffusion potential experiments were used to test whether the pseudin-2 reduced the ability to increase the permeability of SUVs composed of PE/PG (7:3) and PC/CH (8:2). The peptides were mixed at various concentrations with lipid vesicles and pretreated with the fluorescent dye diS-C_3-5 and valinomycin. Fluorescence recovery over time was used to measure the kinetics of dissipation of the diffusion potential induced by the peptides. Pseudin-2 has better ability than melittin in

increasing the permeability of PC/CH vesicles (Figure 11A). Figure 11 show that pseudin-2's permeabilizing activity in PE/PG vesicles is better than PC/CH vesicles. This data is consistent that antimicrobial activity of pseudin-2 toward bacterial cells more potent and fungal cells.

10. Permeabilization of lipid vesicles

The membrane-permeabilizing ability of pseudin-2 was investigated by measuring the release of the fluorescent marker calcein from liposomes. The percentage of calcein leakage 10 min after exposure to the peptide was used as a measure of the membrane permeability enhancing effect of pseudin-2 and melittin (Figure 12). These peptides caused the release of the entrapped marker from all tested liposomes, although the effectiveness were significantly dependent on vesicle composition. This data show that activity of peptides were similar to different membrane-permeabilizing ability. Specially melittin has a little activity for neutral liposomes than pseudin-2. The activity of peptides were against negatively charged liposomes, and the peptide caused an almost total disruption of these vesicles at a concentration (lipid/peptides = 20). However, the variance in the extent of peptide-induced permeabilization of vesicles of any lipid composition at high peptide concentrations was in reality quite low indicating that a threshold peptide/lipid value had been reached.

To gather further clues as to the type and size of membrane damage caused by pseudin-2, we assessed the peptide-induced release of liposome-encapsulated markers of different size. The different lipid vesicles were preloaded with fluorescently labelled dextrans of FD4 (3.9 kDa, 1.8 nm radii), FD10 (9.9 kDa), FD20 (19.8 kDa, 3.3 nm radii), FD40 (40.5 kDa, 4.8 nm radii), FD70 (71.6 kDa, 5 nm radii) and FD500 (530 kDa) and then incubated with increasing amounts of pseudin-2 and melittin. This method allows one to distinguish between the action of a pore-forming peptide, with the possibility to size such pores, and a peptide that acts in a detergent-like manner [57]. The results obtained with pseudin-2 and melittin reveal a marked dependence of peptide-induced leakage on the molecular mass/size of the fluorescent probe (data not

show). Figure 13 show that these peptides revealed concentration-dependent leakage to vesicles. And then psedusin-2 of 10 μM has high activity more than melittin of neutral charged vesicles. Melittin and pseudin-2 were found to release 09% and 100% of FITC-D 4, 48% and 89% of FITC-D 10, 18% and 52% of FITC-D 40, 17% and 32% of FITC-D 70 and 14% and 25% of FITC-D 500, from PC/CH (8:2) at a peptide concentration of 10 μM (lipid/peptide = 30). In the previous data, they have similar antimicrobail activity and forms small pore which can pass calcein and ion. Therefore, the of radii pore size induced by pseudin-2 could explain ~4.8 nm. Pseduin-2 made bigger pore than melittin on zwitterionic vesicles.

11. Electron microscopy analysis

The effects of pseudin-2 on the morphology of *E. coli*, *S. aureus* and *C. albicans* were observed using scanning electron microscopy. When the peptides were applied at concentrations corresponding to 60% MIC, the morphological changes were compared to cells in absence of peptide (Figure 14). In *C. albican*s pseudin-2 caused flabbiness over the entire cell wall, whereas in bacterial cells it induced the burst and aggregation of cells (Figure 14B). This difference may reflect the fact that modes of action of pseudin-2 against various microorganism were expressed by components of cell surface, e.g., cell wall and membrane. On the basis of the electron microscopy studies and spectrometric analysis, pseudin-2 can kill the pathogenic cells and disrupt its membranes by multiple mechanisms of action.

To analyze the morphological changes of melittin-treated vesicles, a comparative examination was carried out before and after the addition of peptide. Electron micrographs revealed that control vesicles appear as spherical or oval bubbles of 50-120 nm (Fig. 15A). Addition of peptide in an appropriate peptide-to-lipid molar ratio (1:20) caused morphological changes (Fig. 15B, C). Figure 15B shows that released micelle-liked structures were induced by peptide, which due to a toroidal pore

mechanism, at critical concentration of peptide. The electron micrograph shows that pseudin-2 forms ring-like structures on PC/CH liposomes. These ring-shaped molecules are either attached to liposomes or are released into solution. The complexes of pseudin-2 bound to membrane were shown to oligomeric form. The results of electron microscopy and chemical cross-linking (Fig. 8) suggest that pseudin-2 forms oligomeric pore complexs. However, in the PE/PG liposomes, no micelle-like structures were observed (Fig. 15C). The remarkable change of negatively charged liposome was not visible, but the size became larger. This result indicate that peptides bind to head group of lipids electrostatically and insert into fatty acid of lipids, and then form small pore as a barrel-stave mechanism. On the basis of the electron microscopy studies of liposomes, we propose that pseudin-2 disrupts membranes by multiple mechanisms of action according to microorganism.

Ⅳ. Discussion

In this study, we showed that pseudin-2 folds into a helical structure at the membrane and then assembles into oligomer. Our results indicate that the mode of action of pseudin-2 changes according to the lipid composition of the liposome (or microorganism). On the basis of the present results, we propose that, in zwitterionic liposomes, pseudin-2 forms a toroidal pore with oligomeric structures at threshold concentration, whereas in negatively charged liposomes, it forms small channel. These findings were analyzed by using the spectrometric studies, biochemical techniques and electron microscopy.

In this studies we found that pseudin-2 has several functional properties. These are: (ⅰ) pseudin-2 has a strong antimicrobial activity but relatively low cytotoxicity; (ⅱ) it can bind to chitin and peptidglycan but not to LPS; (ⅲ) it can form self-oligomers in solution; (ⅳ) it binds and permeates efficiently in negatively charged better than in zwitterionic liposome; (ⅴ) it can form highly aggregate as a multimer when bound to zwitterionic liposome, but as a trimer upon binding to negatively charged liposome; (ⅵ) it is significantly resistant to proteolytic degradation when bound to negatively charged liposome, whereasit is highly susceptible to enzymatic degradation when it bound to zwitterionic charged liposome; (ⅶ) depolarization and dye-leakage assay are concentration-dependent in both liposomes; and (ⅷ) it has different mechanisms according to lipid to peptide ratio and cell types. In the following paragraphs these observations will be discussed in more detail.

Linear antimicrobial peptides that form an amphipathic α-helical structure upon their binding to the bacterial membrane are among the most abundant and widespread in nature. Many studies have demonstrated that alteration of amphipathicity significantly reduces their broad spectrum of antimicrobial activity (19, 44-45). A wheel diagram showed that pseudin-2 could form an amphipathic α-helix. Here, by using CD

spectroscopy, we found that pseudin-2 adopted an α-helical structure in an hydrophobic environment such as 50% TFE and in a mimic environment of the bacterial cell membrane.

Pseudin-2 show increased potency against microorganism but appreciably less cytolytic activity against keratinocytes, fibroblasts and hRBCs. The composition of the bacterial cytoplasmic cell membrane is rich in acidic phospholipids, whereas the plasma membrane of mammalian cells contains a much higher proportion of zwitterionic phosphatidylcholine and sphingomyelin [46]. Here, we confirmed that pseudin-2 has a strong antimicrobial activity and it reveal similar activity with melittin that has been known as requiring very strong activity.

In most microorganisms, the cytoplasmic membrane is surrounded and supported by a cell wall that provides strength, rigidity, and shape. To interact with the membrane, antimicrobial peptides, including melittin must pass through the cell wall. Therefore, if they are unable to bind to the cell wall, they may have less or a complete loss of activity. Although this is an important concept, mechanism studies of cell wall components have been reported only for LPS. Consequently, pseudin-2 is a cationic antimicrobial peptide and it should promote interaction with negatively charged components of microbial surface and increase antimicrobial potency. Here, we show that pseudin-2 can bind to insoluble polysaccharides. In addition, our results indicate that melittin can specifically bind to chitin from yeast and peptidoglycan from Gram-positive bacteria, although can not to LPS from Gram-negative bacteria. In previous report, it demonstrated that melittin could neutralize to LPS, but pseudin-2 showed that could not interact and neutralize in our unpublished data. Can this data explain how pseudin-2 has such a broad antimicrobial activity? We proposes that its antibacterial activity against Gram-negative bacteria is not upon interaction with LPS but with other lipids as another cell barrier.

Selectively, pseudin-2 was less hemolytic at up to 25 μM and it less efficiently than bacteria with negatively-charged membranes. Human RBCs are rich in negatively-charged sialic acid-containing carbohydrate moieties in the form of glycoproteins and glycosphingolipids, which form the glycocalix layer. It is possible that the peptides stick to the negatively charged glycocalix layer and, because of their low capacity to partition within zwitterionic membranes, they cannot diffuse into the membrane. There is also a general consensus that hydrophobic peptide-membrane interactions should determine the hemolytic potency [47]. These studies has been reported previous [22, 48]. In addition we found that pseudin-2 in eukaryotes was less effective than in prokaryotics and it in 10 mM sodium phosphate buffer as low ionic strength buffer also more effective than in PBS as high ionic strength buffer, as shown table 1. Therefore, we confirmed that pseudin-2 is a important antimicrobial peptide with therapeutic potential.

The fluorescence dequenching experiments using Rho-labeled pseudin-2 showed that it oligomerizes in an aqueous solution at low concentration (0.1 μM) more than melittin and it also oligomerizes in liposomes. In addition pseudin-2 was protected from enzymic degradation when bound to negatively liposome but it susceptibility enzymic degradation bound to zwitterionic liposome. Pseudin-2 may already exist to be oligomeric form in solution, so in zwitterionic liposome it may tend to bind weakly. We also found that pseudin-2 exist higher oligomerization in zwitterionic liposome than in negatively charged liposomes, is supported by the chemical cross-linking and FRET analysis. The means that different oligomeric state upon reaching membrane exists.

Next, pseudin-2 ability to dissipate the membrane potential of liposomes and bacteria cells was also tested. We found that pseudin-2 have high potency to permeable negatively charged liposome. It is related to its activities toward bacteria and

mammalian cells. And peptides was tested on their ability to dissipate the membrane potential of bacteria cells. Here, we found a direct correlation between the MICs of peptides against *E. coli* and *S. aureus* and their ability to dissipate membrane potential. Specially, pseudin-2 revealed same dissipate membrane potential against intact *E. coli* and spheloplast of *E. coli* , differently in the case of melittin. Melittin has a comparative high responsibility on outer membrane of bacteria.

Specially, Pseudin-2 and melittin caused the leakage of dextran on the zwitterionic much than negatively charged liposome. And pore size of liposome increasing as the peptide concentration was raised. The FITC-dextran leakage suggests the formation of toroidal pores with an internal diameter of 5 nm on the zwitterionic liposome when liposome : peptide ratio is a 10 : 1. In the high concentration was that it caused small channel formation on the negatively charged liposome and formation of toroidal pore on the zwitterionic liposome. And pseudin-2 has composed a bigger size pore than melittin on the zwitterionic liposome.

Schematic diagrams illustrating the pore formation of peptide *via* the barrel-stave and toroidal models (Figure 16). Given the fact that, in negatively charged vesicle pseudin-2 can span the membrane and thus form a small channel-like transmembrane pore composed of a helical cluster presumed to small barrel-stave pores in the bilayer. On the other hand, it spontaneously interact with PC/cholesterol bilayers, and it forms the toroidal pores, as is previously proposed for melittin and other cationic peptides [49]. This differs from the barrel-stave model in that the peptides are always associated with the lipid head groups, even when they are inserted perpendicularly into the lipid bilayer, and that the lipid monolayer bends continuously through the pore so that the water core is lined by both the peptides and the lipid head groups.

In conclusion, we propose that pseudin-2's mode of action changes according to the lipid composition of the membranes. In membranes made up of zwitterionic

lipids, it forms toroidal pores that progress to micelles, where its effects are mostly due to hydrophobic interactions. In contrast, its effects on negatively charged membranes are mostly governed by electrostatic interactions, and it make small channels.

Table 1. Antimicrobial activity of pseudin-2 and melittin

	MIC (μM)			
	Pseudin-2		Melittin	
	Buffer I †	Buffer II †	Buffer I †	Buffer II †
Bacteria cell G(+)				
L. monocytogenes	1	8	2	2
S. aureus	1	2	2	1
B. subtilis	1	2	2	2
S. epidermidis	2	8	2	16
Bacteria cell G(-)				
E. coli	2	4	2	4
P. aeruginosa	2	8	2	8
S. typhimurium	1	1	1	1
Yeast				
C. albicans	8	16	8	16
T. beigellii	8	16	4	16
Fungi				
A. fumigatus	32	64	32	64
F. oxysporum	64	>64	32	64
A. flavus	32	64	32	64

†; Buffer I and II consist of 10 mM sodium phosphate and PBS, respectively.

Table 2. Cytotoxicity of pseudin-2 and melittin.

Compound	MIC (μM)	Cytotoxicity (IC_{50} μM)			Selectivity (IC_{50}/MIC)		
	E. coli	RBCs	NIH/3T3	HaCat	RBCs	NIH/3T3	HaCaT
Pseudin-2	2	12.5	25	25	6	12	12
Melittin	2	1.5	1.5	1.5	0.75	0.75	0.75

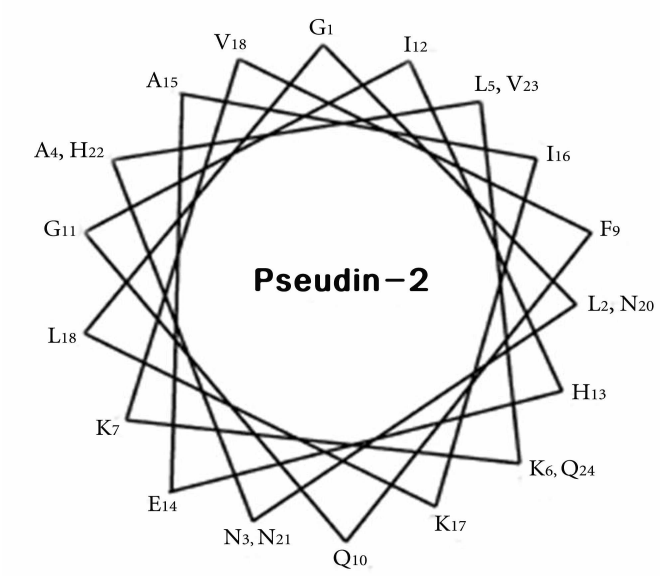

Figure 1. A Schiffer-Edmundson helical wheel projection of the pseudin-2

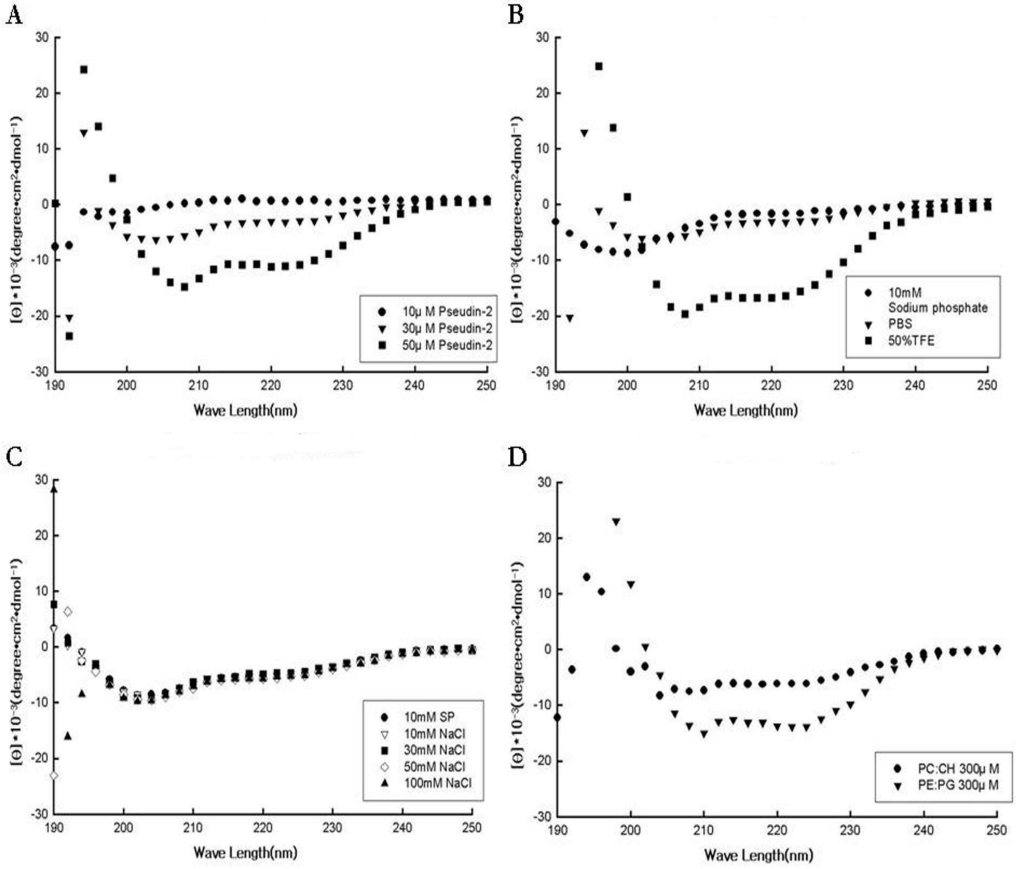

Figure 2. Determination of secondary structure of pseudin-2 in PBS (A), in solution (B), NaCl in sodium phosphate (C), in liposomes (D).

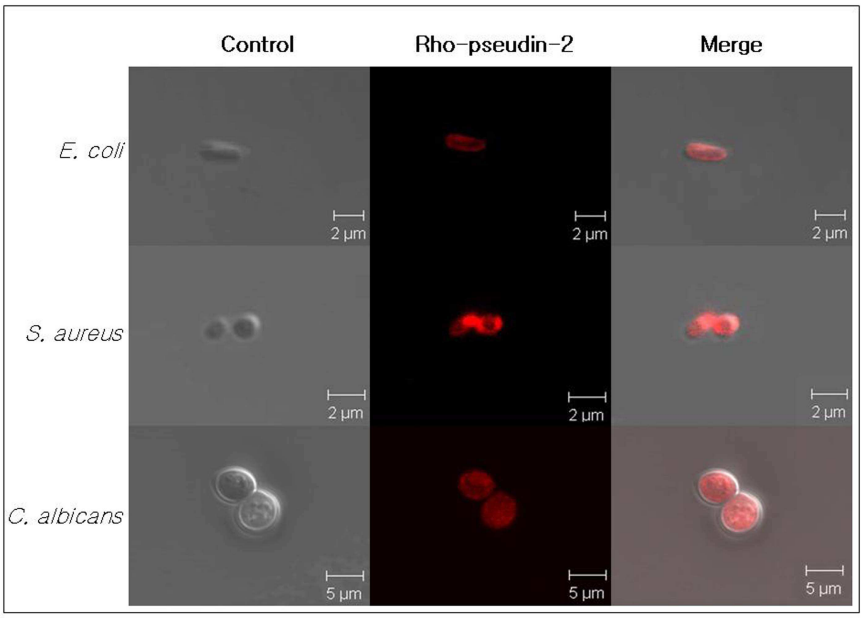

Figure 3. Confocal laser-scanning microscopy images of microbial cells with Rho-labeled pseudin-2.

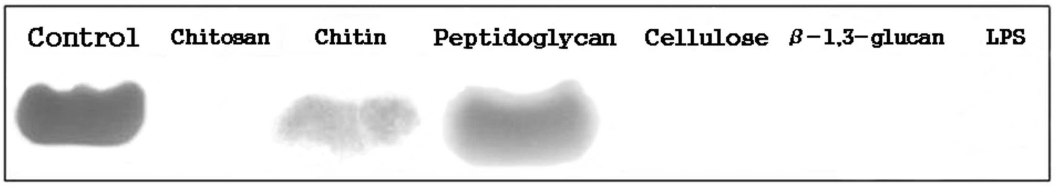

Figure 4. Binding activity of the synthetic peptides. *In vitro* binding assay were carried out using various cell wall components.

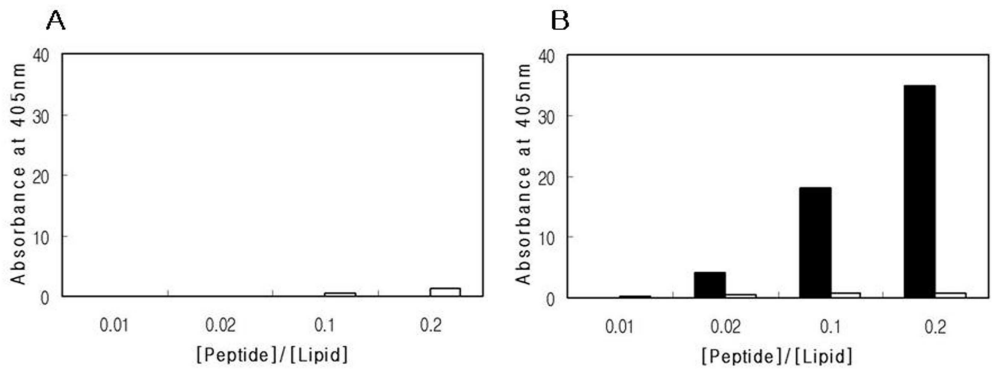

Figure 5. Liposome aggregation measured by turbidity changes. (A) Pseudin-2, (B) Melittin into liposome of 30 μM. Dark squares, PE/PG ; white squres, PC/CH

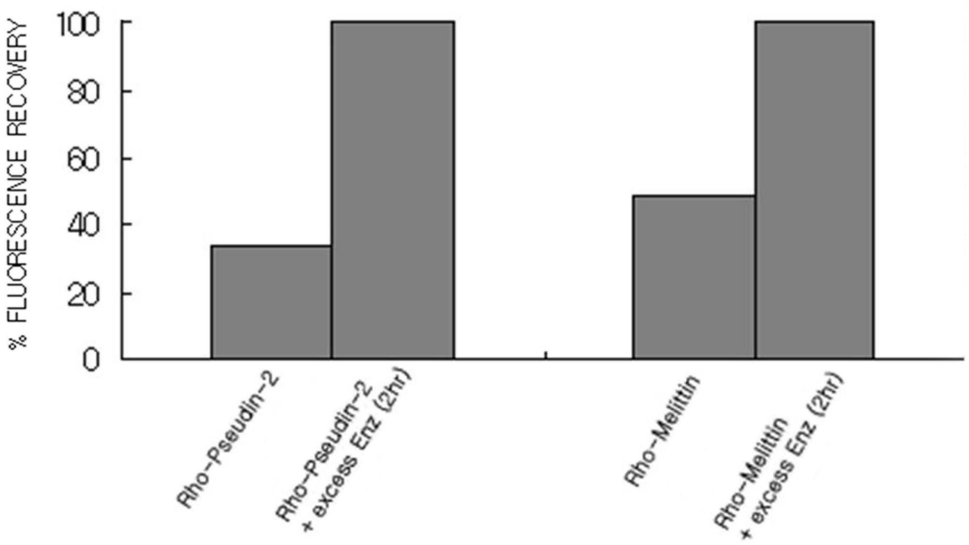

Figure 6. Determination of the aggregation state of pseudiin-2 and melittin in solution. The percentage of fluorescence recovery of Rho-pseudin-2 (0.1 μM) and Rho-melittin (0.1 μM) in PBS in the presence and absence of proteinase K.

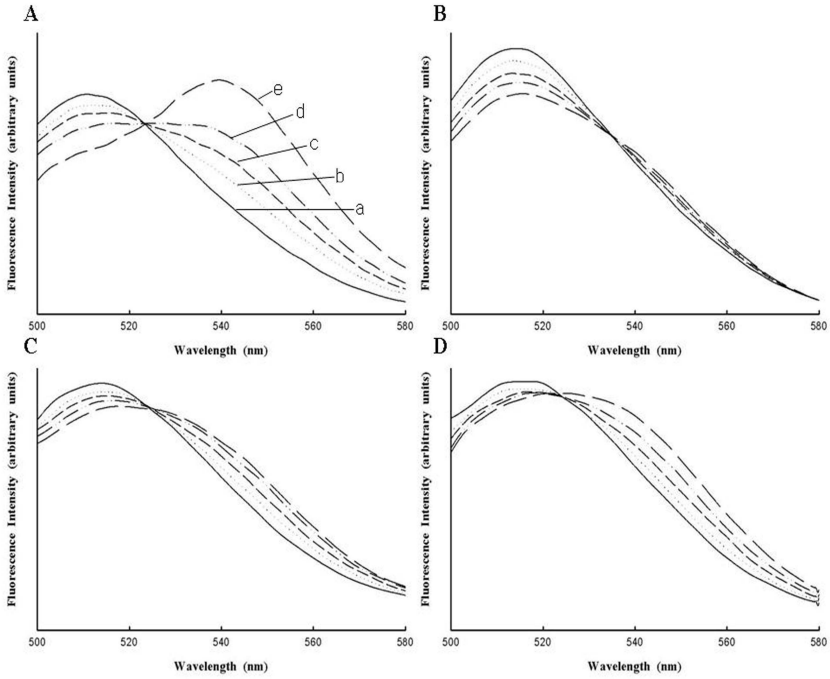

Figure 7. Determination of self-assembly of pseudiin-2 and melittin by studying the fluorescence energy transfer experiments with NBD-labelled donor and Rho-labelled acceptor peptides in the presence of lipid vesicles. The spectra were recorded with the donor peptide alone and in the presence of varying concentrations of acceptor peptide with excitation wavelength set 467 nm. (A) The spectra of NBD-pseudin-2 (0.2 μM) in the prescence of 400 μM of PC/CH (8:2) lipid vesicles alone (a) and with various concentrations of Rho-pseudin-2: b. 0.05 μM; c, 0.1 μM; d, 0.2 μM; e, 0.4 μM. (B) The spectra of NBD-pseudin-2 in PE/PG (7:3). (C) The spectra of NBD-melittin in PC/CH (8:2). (D) The spectra of NBD-melittin in PE/PG (7:3).

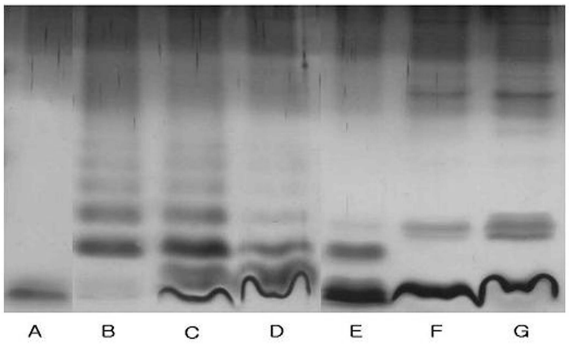

Figure 8. Oligomeric states of pseudin-2 on lipid vesicles. Chemical cross-linked samples were prepared as described in Experimental section. (A), control (only pseudin-2); (B), PC/CH (Molar ratio of peptide and lipids 1:10); (C) PC/CH (1:50); (D) PC/CH (1:100); (E) PE/PG (1:10); (F) PE/PG (1:50); (G) PE/PG (1:100).

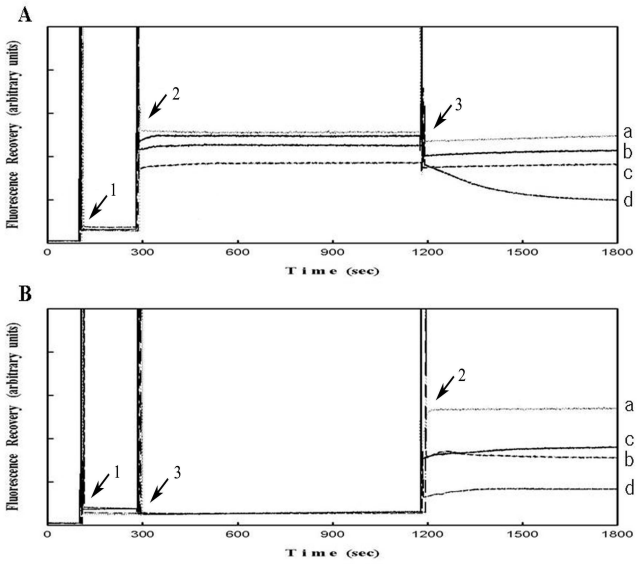

Figure 9. Accessibility of membrane-bound peptides to proteolytic degradation.

(A) Protection of membrane-bound NBD-labelled pseudin-2 and melittin against proteolytic digestion in the presence of negatived and zwitterionic vesicles. (B) In a control experiment proteinase K was added to NBD-labelled psedudin-2 and melittin in buffer prior to the addition of lipid vesicles. The fluorescence intensity of the labelled peptides were monitored at 530 nm with the excitation set at 470 nm. The digestion performed in PBS, pH 7.0. 1,2 and 3 indicated the addition of NBD-peptide (a and c are melittin, b and d are pseudin-2), vesicles (a and b are PE/PG (7:3), c and d are PC/CH (8:2)) and proteinase K, respectively. The concentration of NBD-peptides were 0.2 μM and that of vesicles was fixed at 400 μM.

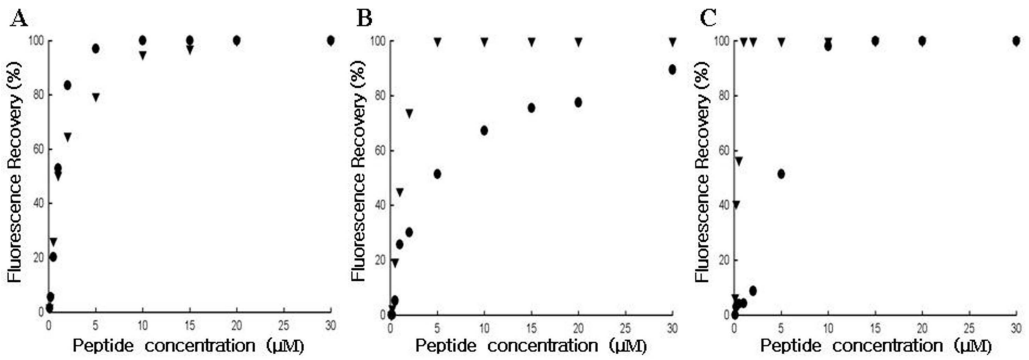

Figure 10. Maximal dissipation of the diffusion potential in bacterial membrane, induced by the peptides. The peptides were added to *E. coli* 25922 (A), spheroplast of *E. coli* 25922 (B) and *S. aureus* 25923 (C) that were pre-equilibrated with the fluorescent dye diS-C_3-5 for 60 min. Fluorescence recovery was measured 1-120 min (at 5-min intervals) after the peptides were mixed with the bacteria, and its maxima was reported. Symbols: circles; Melittin, inverted triangles; Pseudin-2.

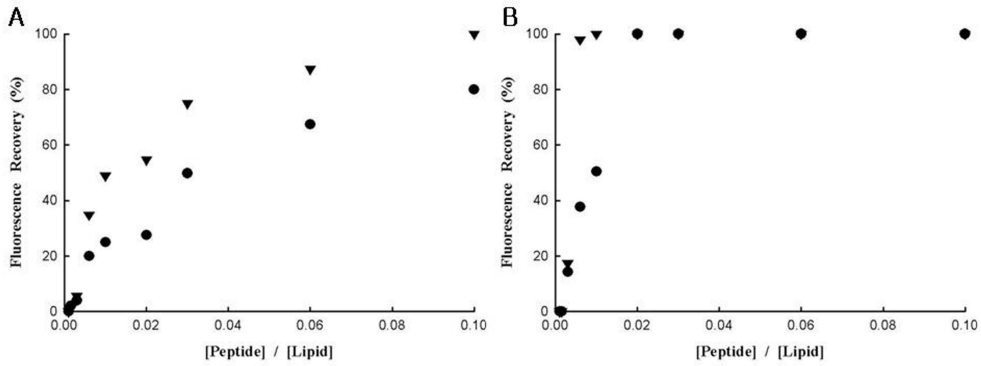

Figure 11. Maximal dissipation of the diffusion potential in vesicles, induced by the peptides. The peptides were added to isotonic K^+-free buffer containing SUVs composed of PC/CH (8:2) (A) or PE/PG (7:3) (B), pre-equilibrated with the fluorescent dye diS-C_3-5 and valinomycin. Fluorescence recovery was measured 5-20 min after the peptides were mixed with the vesicles. Symbols: circles; Melittin, inverted triangles; Pseudin-2.

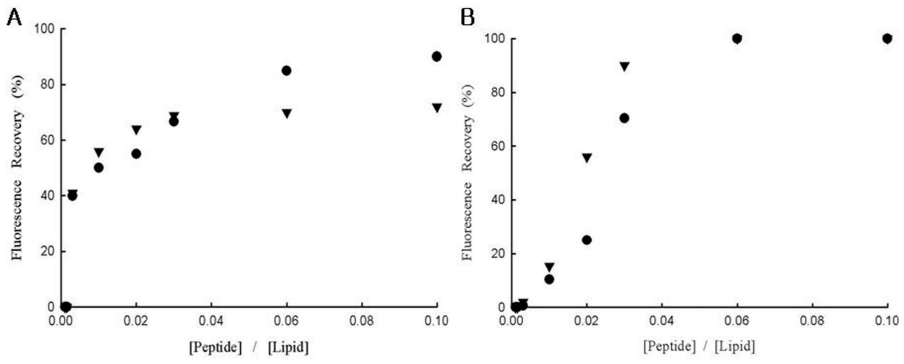

Figure 12. Dependence of calcein leakage from lipid vesicles on pseudin-2 and melittin concentration. Liposomes (final lipid concentration 50 μM in 10 mM HEPES buffer) were incubated in the presence of different concentrations of peptides for up to 10 min at room temperatures. Calcein release was detected fluorimetrically. (A): PC/CH (8:2), (B): PE/PG (7:3). Symbols: circles, Melittin ; squares, Pseudin-2

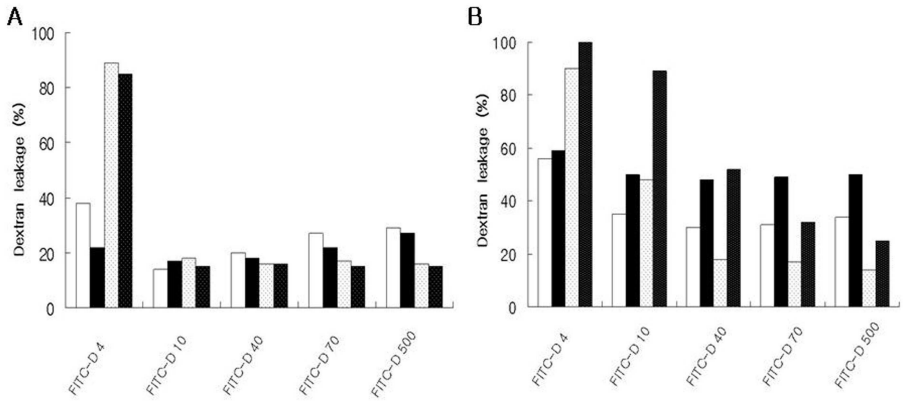

Figure 13. Effect of pseudin-2 on leakage of FITC-D from liposomes. Liposomes (final lipid concentration 300 μM in 2 ml of 10 mM HEPES buffer) PE/PG, first and second column are PC/CH, third and fourth column are PE/PG were incubated in the 1 μM of the peptides (A) and 10 μM of the peptides (B) (Clear columns, Melitin; Dark columns, Pseudin-2) for 10 min at room temperature. Dextran release was detected fluorimetrically.

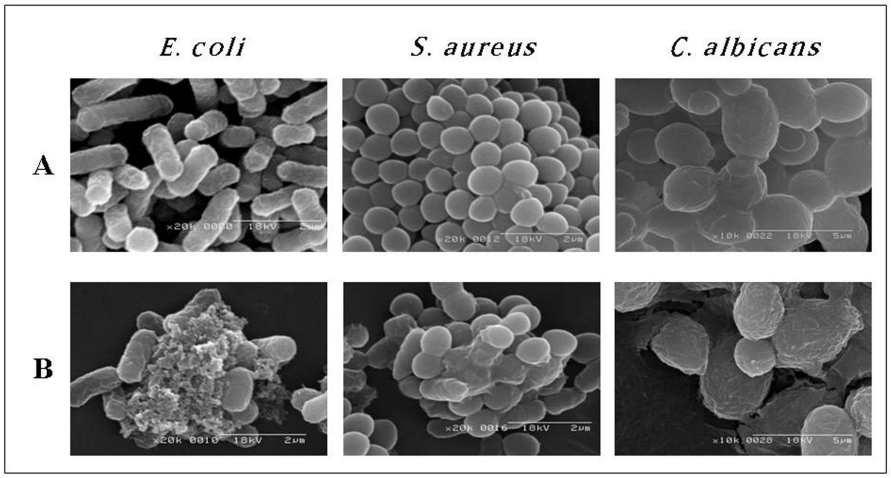

Figure 14. Effect of pseudin-2 on cell morphology. Microbial were treated with pseudin-2 at their MICs. (A) Untreated cells and (B) treated cells.

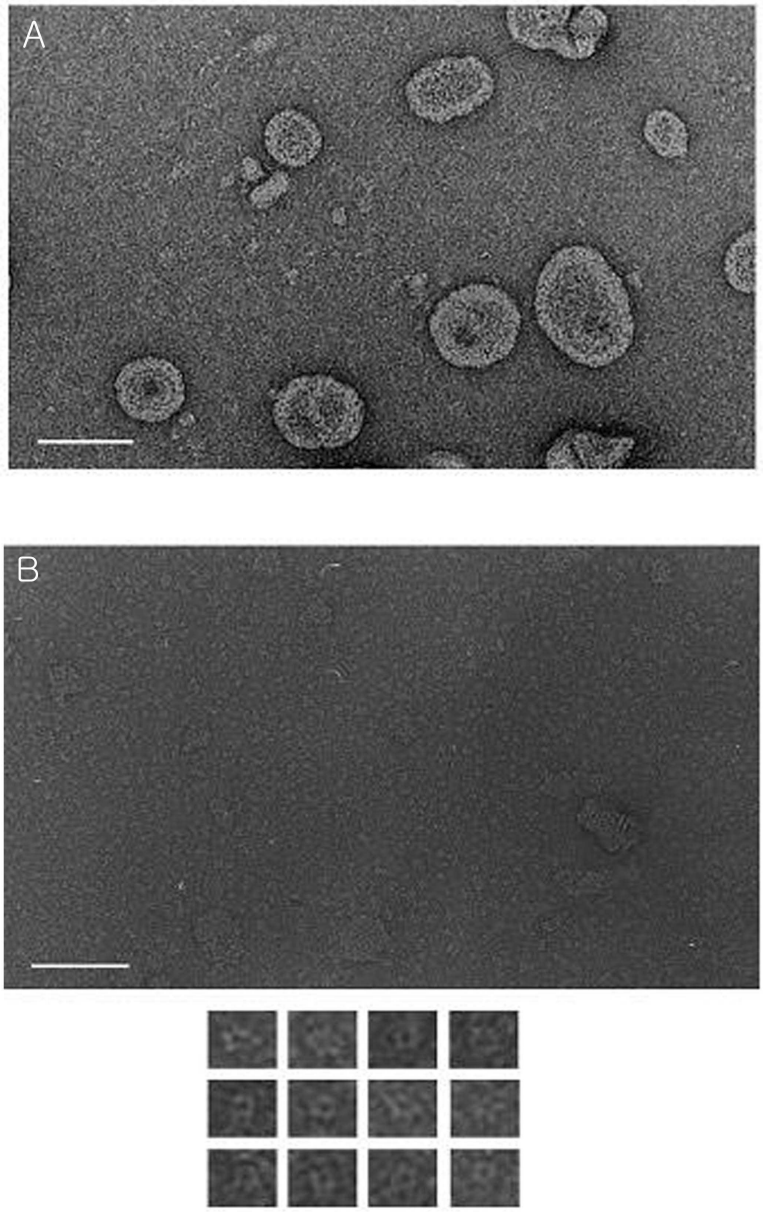
A
B

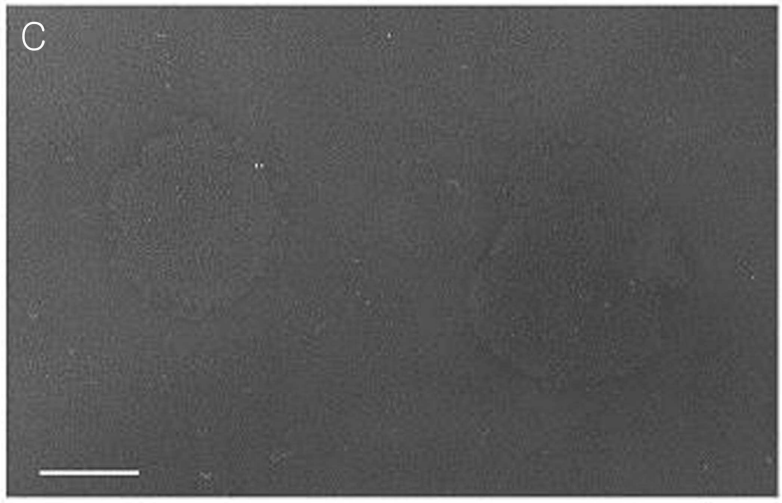

Figure 15. Electron microscopy analysis of morphology changes in PC/CH and PE/PG liposomes. Electron micrographs of a PC/CH liposome without melittin (A), after incubation with 1 μM of melittin for 2 min (B). The galleries of ring-shaped molecules, which are either attached to a liposome or released. PE/PG liposome incubated with 1 μM of melittin for 5 min (C). Scale bars is 100 nm.

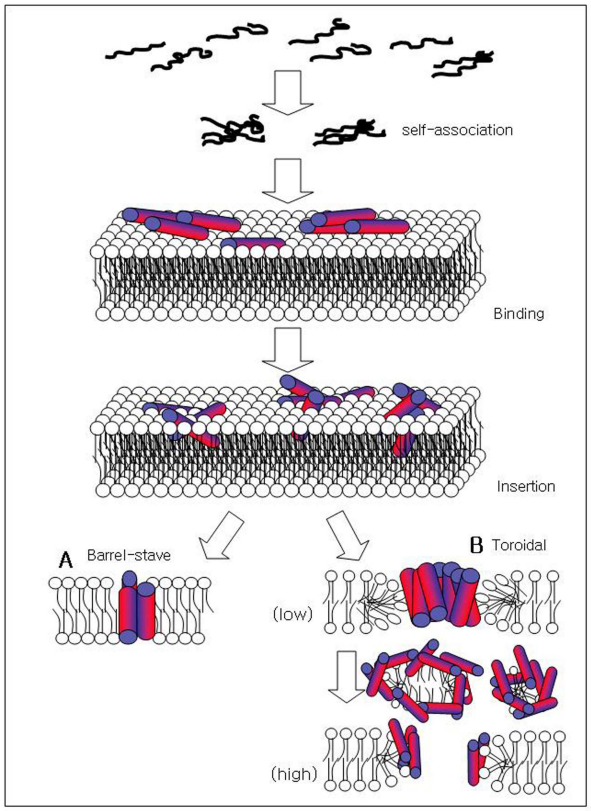

Figure 16. Schematic diagram illustrating the interactions of pseudin-2 with microbial cell membranes. A, the barrel-stave model toward bacterial membrane with negatively charged character. In this model, the attached peptides aggregate and insert into the membrane bilayer so that the hydrophobic peptide regions align with the lipid core region, and the hydrophilic peptide regions form the lining of the pore channel. B, the toroidal model toward fungal membrane with zwitterionic character. In this model, the attached peptides aggregate and induce the lipid monolayers to bend continuously through the pore so that the channel is lined by both the inserted peptides and the lipid head groups.

Ⅴ. References

(1) Zasloff, M. Antimicrobial peptides of multicellular organisms. *Nature*. 2002, **415**, 389-395.

(2) Boman, H.G., and Hultmark, D. Cell-free immunity in insects. *Annu. Rev. Microbiol*. 1987. **41**, 103-126.

(3) Simmaco, M., Mignogna, G., and Barra, D. Antimicrobial peptides from amphibian skin : what do they tell us? *Biopolymers*. 1998, **47**, 435-450.

(4) Zasloff, M., Magainins, a class of antimicrobial peptides from *Xenopus* skin: Isolation, characterization of two active forms and partial cDNA sequence of a precursor. *Proc. Natl. Acad. Sci USA*. 1987, **84**, 5449–5453.

(5) Gibson, B. W., Tang, D., Mandrell, R., Kelly, M., and Spindel, E. R. Bombinin-like peptides with antimicrobial activity from skin secretions of the Asian toad, *Bombina orientalis. J. Biol. Chem*. 1991, **266**, 23103–23111.

(6) Simmaco, M., Barra, D., Chiarini, F., Noviello, L., Melchiorri, P., Kreil, G., and Richter, K. A family of bombinin-related peptides from the skin of *Bombina variegata. Eur. J. Biochem*. 1991, **199**, 217–222.

(7) Matutte, B., Knoop, F. C., and Conlon, J. M. Kassinatuerin-I: A peptide with broad-spectrum antimicrobial activity isolated from the skin of the Hyperoliid frog, *Kassina senegalensis. Biochem. Biophys. Res. Commun*. 2000, **268**, 433–436.

(8) Simmaco, M., Mignogna, G., Barra, D., and Bossa, F. Antimicrobial peptides from

skin secretions of *Rana esculenta. J. Biol. Chem*. 1994, **269**, 11956−11961.

(9) Goraya, J., Wang, Y., Li, Z.,; O''Flaherty, M., Knoop, F. C., Platz, J. E., and Conlon, J. M. Peptides with antimicrobial activity from four different families isolated from the skins of the North American frogs, *Rana luteiventris, Rana berlandieri* and *Rana pipiens. Eur. J. Biochem.* 2000, **267**, 894−900.

(10) Mor, A., Hani, K., and Nicolas, P. The vertebrate peptide antibiotics dermaseptins have overlapping structural features but target specific icroorganisms. *J. Biol. Chem.* 1994, **269**, 31635−31641.

(11) Wechselberger, C. Cloning of cDNAs encoding new peptides of the dermaseptin family. *Biochim. Biophys. Acta*, 1998, **1388**, 279−283.

(12) Steinborner, S. T., Currie, G. J., Bowie, J. H., Wallace, J. C., and Tyler, M. J. New antibiotic caerin 1 peptides from the skin secretion of the Australian tree frog *Litoria chloris.* Comparison of the activities of the caerin 1 peptides from the genus *Litoria*. *J. Pept. Res.* 1998, **51**, 121−126.

(13) Bradford, A. M., Bowie, J. H., Tyler, M. J., and Wallace, J. C. New antibiotic uperin peptides from the dorsal gland of the Australian toadlet, *Uperoleia mjobergi. Aust. J. Chem.* 1996, **49**, 1325−1333.

(14) Boman, H. G. Peptide antibiotics and their role in innate immunity. *Annu. Rev. Immunol*. 1995, **13**, 61-92.

(15) Sawai, M. V., Jia, H. P., Liu, L., Aseyev, V., Wiencek, J. M., McCray, P. B., Jr., Ganz, T., Kearney, W. R., and Tack, B. F. The NMR structure of human beta-defensin-2 reveals a novel alpha-helical segment. *Biochemistry*. 2001, **40**, 3810-3816.

(16) Selsted, M. E., Novotny, M. J., Morris, W. L., Tang, Y. Q., Smith, W., and Cullor, J. S. Indolicidin, a novel bactericidal tridecapeptide amide from neutrophils. *J. Biol. Chem.* 1992, **267**, 4292-4295.

(17) Yong, L., Harroun, T. A., Weiss, T. M., Ding, L. and Huang, H. W. Barrel-stave model or toroidal model ? A case study on melittin pores. *Biophys. J.* 2001, **81**, 1475-1485.

(18) Ben-Efraim, I., and Shai, Y. The structure and organization of synthetic putative membranous segments of ROMK1 channel in phospholipid membranes. *Biophys J.* 1997, **72**, 85-96.

(19) Shai, Y. Mechanism of the binding, insertion and destabilization of phospholipid bilayer membranes by alphahelical antimicrobial and cell non-selective membrane-lytic peptides. *Biochim. Biophys. Acta*. 1999, **1462**, 55−70.

(20) Oren, Z., and Shai, Y. Mode of action of linear amphipathic α-helical antimicrobial peptides. *Biopolymers*. 1998, **47**, 451−463.

(21) Heller, W.T., Waring, A.J., Lehrer, R.I., and Huang, H.W. Multiple states of beta-sheet peptide protegrin in lipid bilayers. *Biochemistry*. 1998, **37**, 17331-17338.

(22) Olson, L,, Soto A,, Knoop. F.C,, and Conlon J.M. Pseudin-2: an antimicrobial peptide with low hemolytic activity from the skin of the paradoxical frog. *Biochem Biophys Res Commun*. 2001, **288**, 1001-1005.

(23) Schiffer, M., and Edmundson. A.B. Use of helical wheels to represent the structures of proteins and to identify segments with helical potential. *Biophys J.* 1967, **7**, 121-135.

(24) Lee, D. G., Kim, H. N., Park, Y., Kim, H. K., Choi, B. H., Choi, C. H. and Hahm, K. S. Design of novel analogue peptides with potent antibiotic activity based on the antimicrobial peptide, HP (2-20), derived from N-terminus of *Helicobacter pylori ribosomal protein L1*. *Biochim. Biophys. Acta*. 2000, **1598**, 185-194.

(25) Rapaport, D., and Shai, Y. Aggregation and organization of pardaxin in phospholipid membranes. A fluorescence energy transfer study *J. Biol. Chem*. 1992, **267**, 6502-6509.

(26) Mayer, L. D., Hope, M. J. and Cullis, P. R. Vesicles of variable sizes produced by a rapid extrusion procedure. *Biochim. Biophys. Acta*. 1986, **858**, 161-168.

(27) Hu, Z., Gogol, E. P., and Lutkenhaus, J. Dynamic assembly of MinD on phospholipid vesicles regulated by ATP and MinE. *Proc. Natl. Acad. Sci. U. S. A.* 2002, **99**, 6761-6766.

(28) Yang, S. T., Shin, S. Y., Lee, C. W., Kim, Y. C., Hahm, K. S., and Kim, J. I. Selective cytotoxicity following Arg-to-Lys substitution in tritrpticin adopting a unique amphipathic turn structure. *FEBS Lett*. 2003, **540**, 229-233.

(29) Blondelle, S.E., and Houghten, R.A. Design of model amphipathic peptides having potent antimicrobial activies. *Biochemistry*. 1992, **31**, 12688-12694.

(30) Wu, C. S., Ikeda, K., and Yang, J. T. Ordered conformation of polypeptides and proteins in acidic dodecyl sulfate solution. *Biochemistry*. 1981, **20**, 566-570.

(31) Asthana, N., Yadav, S. P., and Ghosh, J. K. Dissection of antibacterial and toxic activity of melittin: a leucine zipper motif plays a crucial role in determining its hemolytic activity but not antibacterial activity. *J. Biol Chem*. 2004, **279**, 55042-55050.

(32) Kim, Y. S., Ryu, J. H., Han, S. J., Choi, K. H., Nam, K. B., Jang, I. H., Lemaitre, B., Brey, P.T., and Lee, W. J. Gram-negative bacteria-binding protein, a pattern recognition receptor for lipopolysaccharide and beta-1,3-glucan that mediates the signaling for the induction of innate immune genes in Drosophila melanogaster cells. *J. Biol. Chem*. 2000, **275**, 32721-32727.

(33) Onaderra, M., Mancheno, J. M., Lacadena, J., de los Rios, V., Martinez del Pozo, A. and Gavilanes, J. G. Oligomerization of the cytotoxin alpha-sarcin associated with phospholipid membranes. *Mol. Membr. Biol*. 1997, **15**, 141-144.

(34) Sims, P. J., Waggoner, A. S., Wang, C. H., and Hoffmann, J. R. Studies on the mechanism by which cyanine dyes measure membrane potential in red blood cells and phosphatidylcholine vesicles. *Biochemistry*. 1974, **13**, 3315-3330.

(35) Loew, L. M., Rosenberg, I., Bridge, M., and Gitler, C. Diffusion potential cascade. Convenient detection of transferable membrane pores. *Biochemistry*. 1983, **22**, 837-844.

(36) Ghosh, J. K., Ovadia, M., and Shai, Y. A leucine zipper motif in the ectodomain of Sendai virus fusion protein assembles in solution and in membranes and specifically binds biologically-active peptides and the virus. *Biochemistry*. 1997, **36**, 15451-15462.

(37) Wu, M., Maier, E., Benz, R., and Hancock, R. E. Mechanism of Interaction of Different Classes of Cationic Antimicrobial Peptides with Planar Bilayers and with the Cytoplasmic Membrane of Escherichia coli. *Biochemistry*. 1999, **38**, 7235-724.

(38) Yanagida, N., Uozumi, T., and Beppu, T. Specific excretion of Serratia marcescens protease through the outer membrane of Escherichia coli. *J. Bacteriol*. 1986, **166**, 937-94.

(39) Ghosh, J. K., Peisajovich, S. G., Ovadia, M., and Shai, Y. Serum-induced leakage of liposome contents. *J. Biol. Chem*. 1998, **273**, 27182-27190.

(40) Rajarathnam, K., Hochman, J., Schindler, M., and Ferguson-Miller, S. Interaction of antimicrobial dermaseptin and its fluorescently labeled analogues with phospholipid membranes. *Biochemistry*. 1989, **28**, 3168-3176.

(41) Mangoni, M. L., Rinaldi, A. C., Di Giulio, A., Mignogna, G., Bozzi, A., Barra, D. and Simmaco, M. Structure-function relationships of temporins, small antimicrobial peptides from amphibian skin. *Eur. J. Biochem.* 2000, **267**, 1447-1454.

(42) Park, S. C., Kim, J. Y., Shin, S. O., Jeong, C. Y., Kim, M. H., Shin, S. Y., Cheong, G. W., Park, Y., Hahm, K. S. Investigation of toroidal pore and oligomerization by melittin using transmission electron microscopy. *Biochem Biophys Res Commun*. 2006. **343**, 222-8.

(43) Ladokhin, A. S., Selsted, M. E. and White, S. H. Sizing membrane pores in lipid vesicles byleakage of co-encapsulated markers: pore formation by melittin. *Biophys. J*. 1997. **72,** 1762-1766.

(44) Lehrer, R. I., and Ganz, T. Antimicrobial peptides in mammalian and insect host defence. *Curr. Opin. Immunol.* 1999. **11**, 23–27.

(45) Hancock, R. E., and Diamond, G. The role of cationic antimicrobial peptides in innate host defences. *Trends Microbiol.* 2000. **8**, 402–410.

(46) Yeaman, M. R., and Yount, N. Y. Mechanisms of antimirobial peptide action and resistance. *Pharmacol Rev*. 2003, **55**, 27-55.

(47) Dathe, M., Wieprecht, T., Nikolenko, H., Handel, L., Maloy, L., MacDonald, DL., Beyermann, M.. and Bienert, M. Hydrophobicity, hydrophobic moment and angle subtended by charged residues modulate antibacterial and haemolytic activity of amphipathic helical peptides. *FEBS Lett*. 1997, **403**, 208-212.

(48) Pal T, Sonnevend A, Galadari S, Conlon JM. Design of potent, non-toxic antimicrobial agents based upon the structure of the frog skin peptide, pseudin-2. *Regul Pept.* 2005, **129**, 85-91.

(49) Yang, L., Harroun, T. A., Weiss, T. M., Ding, L. and Huang, H. W. Barrel-Stave Model or Toroidal Model? A Case Study on Melittin Pores. *Biophys. J.* 2001. **81**, 1475–1485.

감사의 글

2년이란 시간동안 좋은 분들을 만나 정말 행복했습니다.
많은 것을 배우고 느끼면서 이 조그만 논문을 만들었습니다. 이제야 학문이 무엇인지 실험이 무엇인지 알았으며 제 자신에 대해서도 많이 알게 되었습니다. 그 동안의 생활을 마음속 깊이 간직하며 새로운 모습을 보이려 합니다.
학문적으로 많은 지도를 해주시고 아버님 같은 모습으로 대해주신 함경수 교수님께 진심으로 감사드립니다. 학부 시절부터 자상한 모습으로 지도해주신 주신 이정섭 교수님께 감사드리며 부족한 저에게 많은 가르침과 관심을 주신 신송엽 교수님께 감사드립니다. 그리고 항상 밝은 모습으로 대해주신 전홍성 교수님께도 감사드립니다.
학부생 시절부터 많은 지도와 관심을 주신 박윤경 교수님, 학문에 대한 열정을 가르쳐 주신 참 좋은 성철이형, 처음부터 지금까지 많은 도움을 주신 고마운 선오형, 실험실 대표 동안 맏언니 진영이, 화장품의 위력을 알게해준 미현이, 선영이, 동물실험실에서 누가 누굴 실험하는지 구분이 안 되는 동기 해균이, 인사가 부담되는 나리 그리고 24시간 실험실 곳곳에서 라이브 방송을 하는 막둥이 진주와 은미 모두에게 감사드립니다. 처음 이곳에 와서 누나 같은 모습으로 챙겨주신 지숙누님 지선누님, 항상 자신감이 넘쳐 술집에서도 자신있게 계산해준 든든한 선배 성진이형, 멋진 선배 규식이형 득수형, 잠 앞에선 순진한 곰으로 변하는 든든한 후배 문영이에게도 고맙습니다. 인생역전을 꿈꾸는 성민이 참 좋은 친구 경호 그리고 우리의 입담꾼 경윤이 대학원 동기 민영이, 남희, 아연이 만룡이, 센터 주당 상용, 홍석, 으뜸, 효정이, 10년을 넘겨버린 소중한 친구 위강, 영남, 주호, 형국, 기종, 낙성, 진욱, 영권, 승민, 세종, 창윤 그리고 초등학교 단짝 호태에게도 고마움 마음을 전합니다.
존경하는 아버님 그리고 사랑하는 어머니 정말 감사합니다. 그리고 든든한 형과 우리 누나에게도 감사드리며 이 논문을 드립니다.

사람은 누구나 저마다
자기의 운명을 손안에 쥐고 있다는 것
그래서 완전히 자기 작품이요,
자기 것이 될 수 있는 생활을
창조하지 않으면 안 된다.

(별지) **저작물 이용 허락서**

학 과	생물신소재	학 번	20057255	과 정	석사
성 명	한글: 정찬영	한문: 鄭 贊 永		영문: Jeong Chan-Young	
주 소	광주 광역시 남구 월산2동 224-2번지				
연락처	E-MAIL: assaview@hanmail.net				
논문제목	한글:***pseudis paradoxa*에서 분리된 항균펩타이드 Pseudin-2의 작용기작에 대한 연구** 영문:**Action Mechanism of Antimicrobial peptide, Pseudin-2 from *Pseudis paradoxa*****				

본인이 저작한 위의 저작물에 대하여 다음과 같은 조건아래 조선대학교가 저작물을 이용할 수 있도록 허락하고 동의합니다. -

다 음

1. 저작물의 DB구축 및 인터넷을 포함한 정보통신망에의 공개를 위한 저작물의 복제, 기억장치에의 저장, 전송 등을 허락함
2. 위의 목적을 위하여 필요한 범위 내에서의 편집·형식상의 변경을 허락함. 다만, 저작물의 내용변경은 금지함.
3. 배포·전송된 저작물의 영리적 목적을 위한 복제, 저장, 전송 등은 금지함.
4. 저작물에 대한 이용기간은 5년으로 하고, 기간종료 3개월 이내에 별도의 의사표시가 없을 경우에는 저작물의 이용기간을 계속 연장함.
5. 해당 저작물의 저작권을 타인에게 양도하거나 또는 출판을 허락을 하였을 경우에는 1개월 이내에 대학에 이를 통보함.
6. 조선대학교는 저작물의 이용허락 이후 해당 저작물로 인하여 발생하는 타인에 의한 권리 침해에 대하여 일체의 법적 책임을 지지 않음
7. 소속대학의 협정기관에 저작물의 제공 및 인터넷 등 정보통신망을 이용한 저작물의 전송·출력을 허락함.

년 월 일

저작자: 정찬영 (서명 또는 인)

조선대학교 총장 귀하